Biomass Conversion and Biorefinery (2024) 14:147–157
https://doi.org/10.1007/s13399-021-02272-5

ORIGINAL ARTICLE

Surface functionalization of graphene oxide by sulfonation method to catalyze the synthesis of furfural from sugarcane bagasse

Le Minh Huong[1,2,3] · Tran Quoc Trung[1,2,3] · Tran Thanh Tuan[1,2,3] · Nguyen Quoc Viet[1,2,3] · Nguyen Minh Dat[1,2,3] · Do Gia Nghiem[1,2,3] · Doan Ba Thinh[1,2,3] · Ninh Thi Tinh[1,2,3] · Doan Thi Yen Oanh[4] · Nguyen Thi Phuong[5] · Hoang Minh Nam[2,3] · Mai Thanh Phong[2,3] · Nguyen Huu Hieu[1,2,3]

Received: 24 September 2021 / Revised: 13 December 2021 / Accepted: 21 December 2021 / Published online: 14 January 2022

Abstract

Recently, graphene-based material as a catalyst has crucially shown a novel strategy in furfural synthesis from biomass resources. In this study, sulfonated graphene oxide (SGO) was studied within five different graphene oxide to sulfanilic acid mass ratios of 1:1.5, 1:2.0, 1:2.5, 1:3.0, and 1:3.5 for facile synthesis of furfural from sugarcane bagasse. The structural investigation of those samples was proceeded through Fourier transform infrared spectroscopy, Raman spectroscopy, and energy-dispersive X-ray spectroscopy. The appropriate sample with the sulfur mass percentage of 3.51 %, corresponding to the ratio of 1:3.5, gives out the highest furfural yield was then, conducted with X-ray diffraction, Scanning electron microscopy, Transmission electron microscopy, and Brunauer-Emmett-Teller for further morphological analysis. The influence of catalyst dose, reaction temperature, and time on the yield of furfural using this catalyst revealed that under reaction conditions of 190 °C for 90 min, reaction in a low dose of 5 wt% of SGO solution gave out the highest conversion of furfural (20.6 %). According to the results, SGO showed high application potential for the synthesis of furfural from sugarcane bagasse.

Keywords Graphene-based material · Sulfonated graphene oxide · Furfural · Sugarcane bagasse

1 Introduction

The extremely rapid depletion of fossil fuel supplies has led to the search for potential alternatives. Hemicellulosic biomass has emerged as one of the most important alternative resources in a variety of industries nowadays. Among a variety of products that can be produced from these feedstocks, furfural ($C_5H_4O_2$) is regarded as a potential organic compound for a lot of applications such as pharmaceutical, food, or petrochemical industries [1, 2]. Xylose, a 5-carbon sugar, found in a variety of agricultural wastes, may be used for synthesizing this heterocyclic molecule, which involves hydrolysis of agricultural surpluses to xylose, subsequently dehydration of xylose to furfural with acidic catalysis [3].

There has been a host of researches carried out to obtain furfural. One of the common methods is using homogeneous acids as catalysts (H_2SO_4, HCl, and H_3PO_4) which results in a lot of negative effects such as contamination, health risks, or equipment corrosion [4, 5]. Additionally, furfural can be also synthesized without the addition of catalysts, owing to an autocatalytic reaction mechanism: when xylose is heated, organic acids are formed, which can function as homogenous catalysts in the synthesis of furfural. Nevertheless, these processes involve the occurrence side reactions, which significantly diminish the production yield and lead to an abundance of environmental issues [6]. As a consequence, research into novel chemical technologies to enhance the

✉ Nguyen Huu Hieu
nhhieubk@hcmut.edu.vn

1 VNU-HCM, Key Laboratory of Chemical Engineering and Petroleum Processing (Key CEPP Lab), Ho Chi Minh City University of Technology (HCMUT), 268 Ly Thuong Kiet Street, District 10, Ho Chi Minh City, Vietnam

2 Faculty of Chemical Engineering, Ho Chi Minh City University of Technology (HCMUT), 268 Ly Thuong Kiet Street, District 10, Ho Chi Minh City, Vietnam

3 Vietnam National University Ho Chi Minh City (VNU-HCM), Linh Trung Ward, Thu Duc City, Ho Chi Minh City, Vietnam

4 Publishing House for Science & Technology, 18 Hoang Quoc Viet, Cay Giay, Ha Noi, Vietnam

5 Ho Chi Minh City University of Food Industry, 140 Le Trong Tan Street, Tay Thanh Ward, Tan Phu District, Ho Chi Minh City, Vietnam

efficiency of furfural production while minimizing environmental effects is critical for the growth of furan-based chemical companies.

One of the promising methods for efficient furfural production is using heterogeneous catalysts, which are environmentally friendly and can be easily reusable as compared to homogeneous ones [7]. These types of catalysts have been playing a vital role in the conversion of xylose to furfural. Particularly, grafting sulfonic groups (–SO_3H) are broadly used due to high production efficiency and powerful catalysis performance [8]. However, due to the limited accessible active site of these solid acid catalysts and high mass transfer resistance, the catalysis efficiency is significantly hindered. Carbonaceous nanomaterials, especially graphene oxide (GO), which is usually used to immobilize active species or as a catalyst, can be one of the promising agents to tackle the above phenomenon. It has an variety of outstanding properties such as good conductivity a large specific surface area [9]. Besides, GO also provides a lot of oxygen-containing functional groups, such as epoxy, hydroxyl, and carboxyl [10], which make it become one of the powerful catalysts for many reactions [11]. Several kinds of research have shown that GO and its derivatives, sulfonate graphene oxide (SGO), can be used as eco-friendly and economical carbonaceous catalysts in many acid-catalyzed chemical reactions [12]. Hence, the presence of SGO as acidic catalysts can dramatically enhance the efficiency of furfural production without environmental consequences.

Furthermore, homogeneous catalysts such as metal salts, mineral acids, and enzymes, as well as heterogeneous catalysts in organic solvents such as dimethyl sulfoxide and ionic liquids, are the most frequent methods for carrying out furfural conversion processes [13]. In these reaction systems, however, hazardous organic solvents, severe reaction conditions, and expensive ionic liquid solvents are generally needed. Recently, green catalytic reactions are more favorable, and these processes require the utilization of ecologically acceptable and long-lasting catalytic processes, which need the use of non-toxic and low-cost solvents. Water is the ideal replacement for a green solvent to support the furfural production, which could avoid the use of toxic and hazardous solvents and reduce waste formation, thereby adhering to the most fundamental criteria of green chemistry.

In the study, SGO was prepared by Samulski's method, which was initially used to enhance the hydrophilicity of reduced graphene oxide through the attachment of –$C_6H_4SO_3H$ in 2007 [14]. The obtained solid catalyst was directly used as a catalyst to synthesize furfural from sugarcane bagasse. The material was carried out with 5 precursor mass ratios, which is analyzed characterization using modern analytical. Then, a suitable sample with the greatest furfural production was continuously investigated according to 3 factors: the amount of catalyst, reaction temperature, and time. The mechanism of the hydrolysis reaction from the biomass source to the furfural product was also briefly discussed.

2 Materials and methods

2.1 Materials and chemicals

Furfural ($C_5H_4O_2$) was purchased from Fisher Scientific Co. Ltd, Switzerland; graphite powder (particle size < 20 µm) was purchased from Sigma Aldrich Co. Ltd, USA; sulfuric acid (H_2SO_4), phosphoric acid (H_3PO_4), potassium permanganate ($KMnO_4$), hydrogen peroxide (H_2O_2), sodium hydroxide (NaOH), hydrochloric acid (HCl), sulfanilic acid ($C_6H_7NO_3S$), sodium nitrite ($NaNO_2$), and ethanol (C_2H_5OH) were purchased from Xilong Scientific Co. Ltd, China. All chemicals were used without any further purification. Sugarcane bagasse was collected from Dong Nai, Vietnam.

2.2 Synthesis of catalyst

2.2.1 Synthesis of GO

GO was synthesized via the improved Hummers' method [15]. Briefly, 3 g of graphite was added to a 400 mL mixture of concentrated H_2SO_4 and H_3PO_4 with the volumetric ratio of 9:1. Afterward, 18 g of $KMnO_4$ was added gradually to the mixture while kept stirred at below 10 °C. The mixture was then heated to 50 °C and stirred for 12 h. Subsequently, 500 mL of distilled water and 15 mL of 30 % H_2O_2 were then added to the mixture after being cooled down to room temperature, and a change in color from brown to white yellow upon the addition of H_2O_2 was observed. The resultants were purified by centrifugation at a speed of 2000 rounds/min and rinsed with water until the desired pH of 6 was achieved. The obtained solid was dried at 50 °C, dispersed in distilled water with a concentration of 5 g/L, and ultrasonicated for 12 h. The suspension was then centrifuged and dried at 50 °C to obtain GO.

2.2.2 Synthesis of SGO

The as-prepared GO was applied to synthesize SGO by Samulski's method as shown in Figure 1 [14]. Briefly, sulfanilic acid (SA) was dispersed in 5 % NaOH. Afterward, $NaNO_2$ was added to the mixture, stirred for 10 min, and transported in an ice bath. The solution was then added with 1 N HCl and stirred for another 15 min to obtain a homogeneous solution. The mixture was added into GO solution at 0–5 °C and stirred for 4 h. The suspension was washed with distilled water, centrifuged, and dried at 50 °C to obtain SGO. The

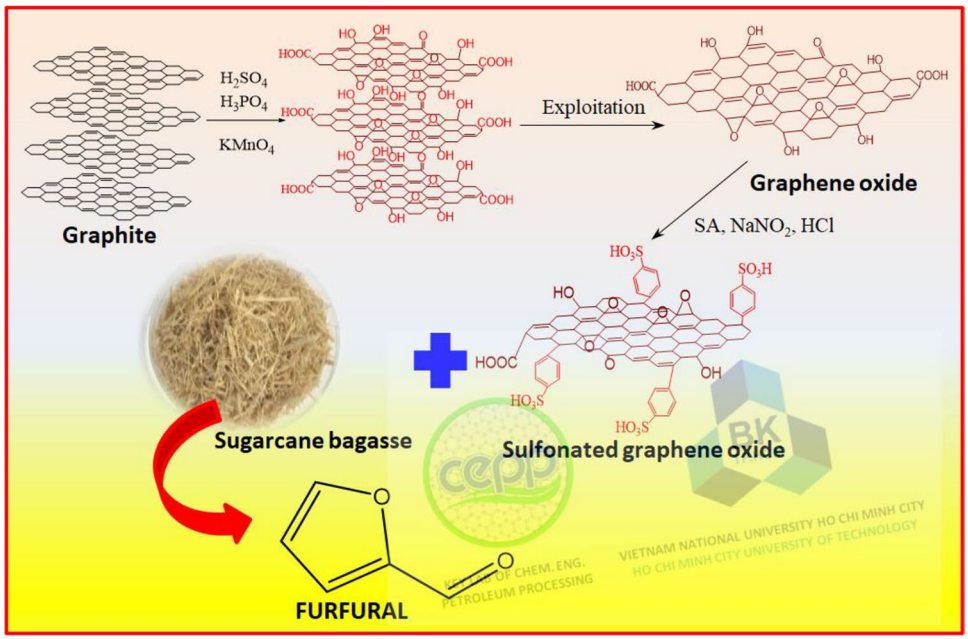

Fig. 1 Schematic pathway of SGO and furfural synthesis

influence of precursor ratio on the structure and catalytic performance of SGO was investigated. SGO samples synthesized from various precursor ratios are demonstrated in Table 1.

2.3 Catalytic conversion of sugarcane bagasse into furfural

The synthesis of furfural consisted of two steps, namely, (1) extraction of hemicellulose from sugarcane bagasse and (2) hydrolysis of hemicellulose to obtain xylose and dehydration of xylose to furfural.

2.3.1 Extraction of hemicellulose from sugarcane bagasse

Sugarcane bagasse was grounded, washed with hot water and ethanol, and dried at 50 °C. Then, 5 g of dried sugarcane bagasse was added into 75 mL of 2 N NaOH solution within stirring at 90 °C for 2 h. The obtained solution was filtered and washed with 20 mL of NaOH and 20 mL of 0.1 N HCl solution. The filtered solution was evaporated until half remained, followed by the adjustment of pH to 4. Ethanol was added slowly until precipitation was observed. The solution was then filtered and washed with ethanol to obtain hemicellulose.

2.3.2 Synthesis of furfural

Furfural was synthesized from hemicellulose via hydrolysis and dehydration [12]. Briefly, SGO suspension was added into the hemicellulose solution. The mixture was then sealed in high-pressure reactor Parr 4848 under constant stirring at set temperature and time. The resultant vapor was condensed and cooled to room temperature. The obtained solution was quantitatively analyzed by UV-vis spectrometer (Dual-FL, Horiba) at the wavelength of 278 nm for furfural content. The influence of SGO dose (2–8%), reaction temperature (150–230 °C), and reaction time (50–130 min) on furfural yield were studied step by step.

Furfural yield H (%) is calculated based on the ratio of the mass of furfural produced and mass of sugarcane bagasse used as described in Equation (1):

$$\mathrm{H}(\%) = \frac{\text{mass of furfural produced (g)}}{\text{mass of used sugarcane bagasse (g)}} \times 100 \quad (1)$$

Table 1 Experimental setup for SGO precursor mass ratio investigation

Samples	GO (mL)	SA (g)	$NaNO_2$ (g)	NaOH (mL)	HCl (mL)	H_2O (mL)
SGO-1	200	1.5	0.6	7.2	18	50
SGO-2	200	2.0	0.8	9.6	24	50
SGO-3	200	2.5	1.0	12.0	30	50
SGO-4	200	3.0	1.2	14.4	36	50
SGO-5	200	3.5	1.4	16.8	42	50

2.4 Characterization

Scanning electron microscope (SEM) images were used to study the morphologies of the synthesized nanocomposite by using S-4800, Hitachi, Japan, with the accelerating voltage of 10 kV, magnification of 5,000 to 300,000×, resolution of 0.2 nm for high contrast polepiece, and 0.14 nm for high-resolution polepiece and JEM-1400, JEOL, Japan, with the maximum accelerating voltage of 120 kV with the magnification of 800,000× and CCD systems for image capture. Fourier transform infrared spectroscopy (FTIR) was measured by using Alpha-E, Bruker Optik GmbH, Ettlingen, Germany, with potassium bromide (KBr) pellets in mid-infrared range (400–4000 cm^{-1}) with a resolution of 0.2 cm^{-1} and standard deviation of 0.1 % T. Raman spectra were used to study the defects of SGO by using Labram 300, Jobin Yvon, Japan. X-ray diffraction (XRD) was carried out in D2 Phaser, Brucker, Germany with Cu-K_α radiation ($\lambda = 0.1541$ cm^{-1}), 2θ scan range between 5 and 80 °, scanning speed of 1 °/s, step size of 0.02. Brunauer-Emmett-Teller (BET) specific surface area was measured by BET adsorption/desorption isotherm of N_2 at 77.35 K and 756 mmHg by utilizing NOVA 2200e, Quantachrome, America. Energy-dispersive X-ray spectroscopy (EDX) was recorded by using JMS, JEOL, Japan, with operating parameters of Wolfram cathode, accelerating voltage between 0.5 and 30 kV, and resolution of 3 nm at 30 kV and 1 nm at 15 kV. UV-visible spectrophotometry (UV-vis) was performed on Horiba Dual FL, Japan, to determine the concentration of furfural post-reaction.

3 Results and discussion

3.1 Influence of precursor ratio on the characteristic and catalytic performance of SGO

As shown in Figure 2a, the presence of functional groups of the synthesized samples is analyzed via FTIR spectra. FTIR spectra of GO show absorption peak at 1731, 1403, and 1128 cm^{-1} corresponding to C=O, C–OH, and C–O–C groups, respectively [16]. In particular, it could be observed that there is a distinctive peak at 3000–3700 cm^{-1} characterized by the vibration of –OH. These results can be explained that Gi has been oxidized, leading to the attachment of oxygen-containing functional groups in the structure. Besides, the FTIR spectrum of GO also has the distinctive peak of the C=C bond at the 1613 cm^{-1}, which is a characteristic bond for the carbon network of graphene-based materials [17]. FTIR spectra of SGO materials have fluctuations similarly to those of GO. Besides that, the oscillation peaks at 1352, 1218, and 1071 cm^{-1} demonstrated the successful functionalization of $–SO_3H$ and O=S=O in the structure of SGO [12]. The intensity of these peaks increased with the amount of SA used for preparing SGO-1 to SGO-5. This proved that the efficiency of the sulfonation increases gradually with the dose of SA. The success in sulfonation of graphene oxide is further demonstrated by structural and morphological studies.

Raman spectra of GO material and SGO samples are presented in Figure 2b. GO has two characteristic D and G bands centered at 1330.04 and 1593.41 cm^{-1}, respectively [18]. The former is observed at about 1327–1330 cm^{-1}, while the latter shows a peak at the position of about 1590–1600 cm^{-1}, which is consistent with previous studies [19]. GO has a much lower I_D/I_G ratio than samples synthesized by conventional methods, confirming the role of H_3PO_4 in controlling the excessive oxidation and reducing defects in the carbon network [12]. Despite the presence of flaws in the lattice, the catalytic material SGO-5 has the same structure as GO. The I_D/I_G values of 5 samples are reported in Table 2, demonstrating that the defect in the structure of SGO material is higher than that of GO [11]. This can be explained by the covalent bonding of $–C_6H_4SO_3H$ ($–PhSO_3H$) and oxygen-containing functional groups, breaking the C=C bonds in the graphene structure, and altering several atoms C in sp^2 hybrid state to sp^3. Due to the increase in the intensity

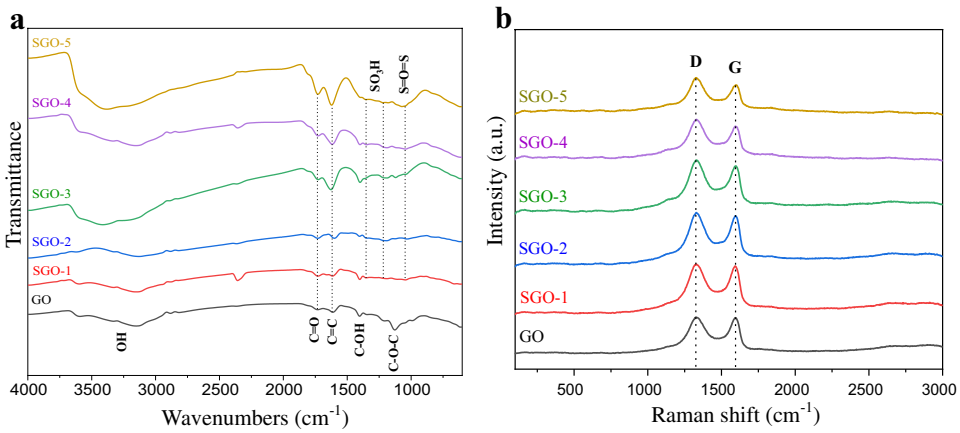

Fig. 2 **a** FTIR and **b** Raman spectra of GO and 5 researching SGO samples

of D and decrease in that of the G peak, the ratio of I_D/I_G increases. In addition, increasing I_D/I_G values of SGO samples showed that the sulfonation efficiency increased when the amount of SA precursors involved in the GO reaction increased.

The successful attachment of sulfonate $–SO_3H$ groups to the GO substrate is further verified through the results of elemental composition analysis in the materials as shown in Table 2. The results showed that the presence of element S in the SGO samples and the mass percentage of S element increased gradually, corresponding to the decrease in the C/S ratio from SGO-1 to SGO-5.

As demonstrated in Figure 3, diluted furfural (10 mg/L) solution demonstrated a distinctive absorption peak at 278 nm. The synthesized furfural using GO and SGO catalysts displayed the same peak as pure furfural with varied absorbance strength. The results in Table 2 show that the furfural efficiency as using the catalyst of SGO samples is much higher than as using GO (1.5–2 times). This proved that the additional attachment of $–SO_3H$ groups onto GO increases the acidity of the material many times, although GO still has acidic functional groups like –OH or –COOH [20]. By the results of the elemental composition analysis, an increase in the composition of sulfonate groups increased gradually as % S in these samples increased in the order of 1.39, 1.76, 2.09, 2.50, and 3.51 %, corresponding to an increase in catalytic efficiency of 7.9, 9.2, 9.6, 9.9, and 10.2 %, from samples SGO-1 to SGO-5, respectively, which is similar to the obtained results of UV-vis analysis of the post-reaction solution. For the solid catalysis in furfural synthesis, the acidity depended on the amount of acidic functional groups in the structure of the material plays as the main factor in affecting furfural synthesis efficiency [21]. With the most effective catalytic ability to catalyze furfural formation, SGO-5 synthesized with a GO:SA precursor ratio of 1:3.5 was chosen as the main catalyst material used in this study. SGO-5 material continues to be analyzed more carefully in terms of structural–morphological characteristics and its application as a catalyst for the investigation of factors affecting the efficiency of furfural synthesis.

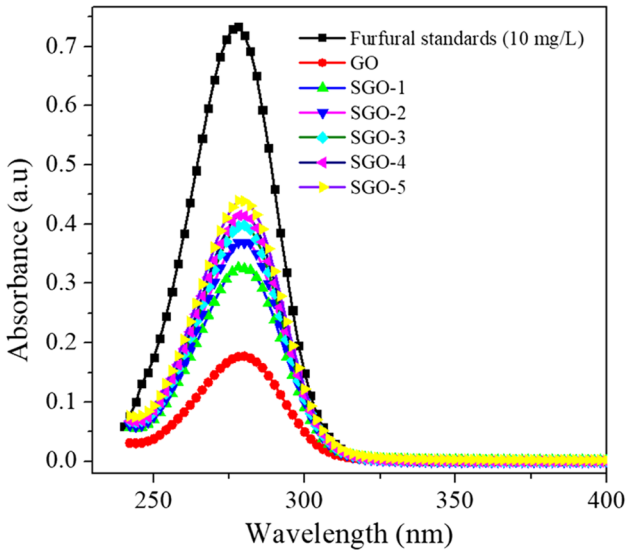

Fig. 3 UV-vis spectra furfural standard and production (reaction condition: 2 % SGO, 190 °C, and 90 min, 1:10 dilution)

As shown in Figure 4, the crystal structure of GO and SGO-5 was reflected by XRD analysis. The diffraction peak of the crystal plane (002) at $2\theta = 11.49$ °, which is consistent with interlayer spacing $d_{(002)} = 1.139$ nm. This indicates the presence of oxygenated functional groups that have bonded to the GO surface, increasing the distance between the monolayers when compared to pristine graphite [15, 22]. The XRD pattern of SGO-5 is similar to that of GO, but the diffraction peak (002) shifted to $2\theta = 10.53$ ° ($d_{(002)} = 1.243$ nm). This result demonstrates that the functionalization of $–SO_3H$ does not have a significant effect on the crystal structure of GO [12]. The increase in the interlayer spacing indicates that the functionalization of the sulfonic group could help minimize the restacking of GO sheets.

As indicated in Figure 5, SEM images of GO and SGO-5 demonstrated the randomly stacked and overlapped thin GO sheets with numerous wrinkles and folds. Furthermore, the SEM image of SGO-5 also showed that the structure of GO remained intact after the sulfonation [23].

Table 2 Element analysis, Raman intensity ratio, and furfural yield of GO and 5 researching SGO samples

Samples	Mass (%)			C/S ratios	Atomic (%)			C/S ratios	I_D/I_G	Furfural yield (%)*
	C	O	S		C	O	S			
GO	49.15	50.85	–	–	56.28	43.72	–	–	1.010	4.8
SGO-1	52.00	46.61	1.39	37.41	59.42	39.99	0.59	100.71	1.027	7.9
SGO-2	50.70	47.54	1.76	28.81	58.24	41.00	0.76	76.63	1.046	9.2
SGO-3	51.54	46.37	2.09	24.66	59.15	39.95	0.90	65.72	1.075	9.6
SGO-4	48.97	48.52	2.50	19.59	56.72	42.19	1.09	52.04	1.109	9.9
SGO-5	52.54	43.95	3.51	14.97	60.49	37.99	1.52	39.79	1.131	10.2

*Reaction condition: 2 % SGO, 190 °C, and 90 min

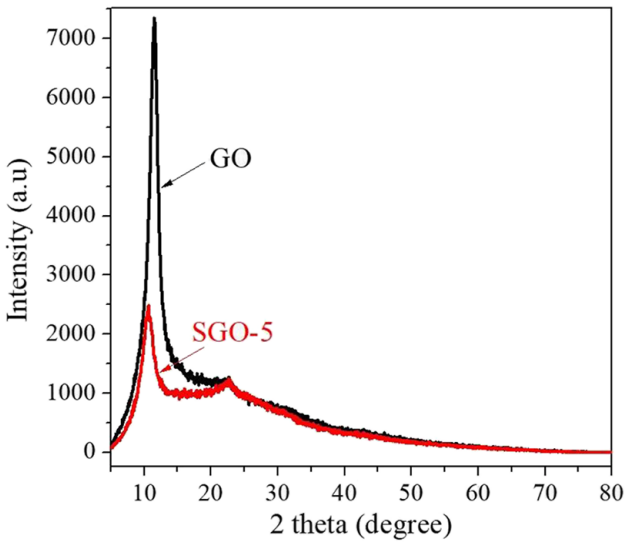

Fig. 4 XRD patterns GO and SGO-5

Figure 6 shows TEM images analyzing the morphologies of GO and SGO-5 which are similar to the analysis results of SEM images; wrinkles and folds show that GO and SGO-5 are made up of many 2-dimensional monolayers linked together by interactions between oxygen-containing functional groups or by π–π interaction [24]. In addition, the dark areas on the TEM image of SGO-5 are more transparent than the GO, showing less stacking of single-layer sheets [20]. This demonstrates that when functionalization of $–PhSO_3H$, the separation of each layer of SGO material is more effective than GO material.

EDX spectra of GO and SGO-5 are shown in Figure 7. Despite the signals of elements C and O, SGO-5 also gave the signal of element S, which shows the agreement with the results of FTIR analysis, when the $–PhSO_3H$ groups were successfully functionalized to the GO structure [12, 20]. Furthermore, a weak signal of element S could be detected in the EDX spectrum of GO as there have been reported the formation of organosulfur functional groups on the surface of GO when the improved Hummer' method is used [25, 26].

Specific surface areas BET of GO and SGO-5 material are 91.1 and 88.05 m^2/g, respectively. The specific surface area of SGO-5 is slightly lower than that of GO that is related to the functionalization of sulfonate groups onto GO sheets [27]. Furthermore, the drying of GO sheets could lead to the stacking of GO sheets, subsequently, explaining the

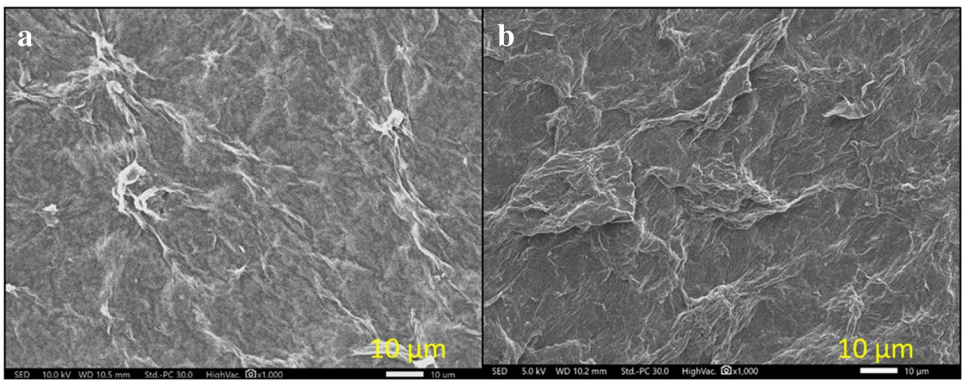

Fig. 5 SEM images with a different magnification of **a** GO and **b** SGO-5

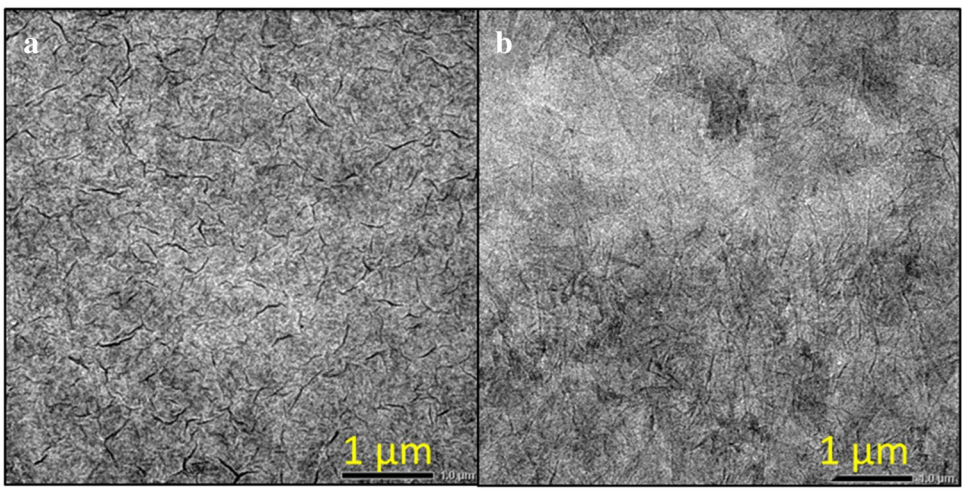

Fig. 6 TEM images with a different magnification of **a** GO and **b** SGO-5

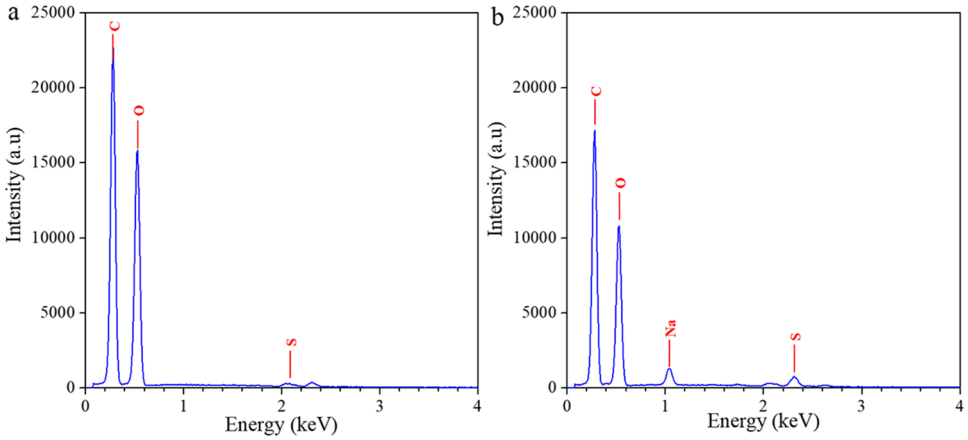

Fig. 7 EDX spectra of **a** GO and **b** SGO-5

Table 3 Specific surface area and pore size of some reported materials

Material	Specific surface area (m^2/g)	Pore size (nm)	Reference
GO	91.1	2	[This study]
SGO-5	88.05	2.8	[This study]
S-rGO	900	4.5	[28]
rGO	300	5.5	[28]
AC-SO_3H	753	4.1	[29]
GO-SO_3H	217	15	[29]

low specific surface area of GO and SGO solid catalysts. The analytical results of the specific surface area and pore size of the materials are lower than the previous studies as shown in Table 3. This can be explained by the fact that SGO still retains the layered structure after the synthesis process, leading to the number of cross-linking between the GO plates to create lower porosity than the finish cladding materials.

3.2 Influences of reaction conditions on the catalytic performance of SGO

Hemicellulose after being isolated was dispersed in deionized water and used as a starting material for furfural synthesis. The SGO nanomaterial for production of furfural was conducted via 2–8 wt%. The results in Figure 8a witnesses a maximum yield of 20.6 % as the catalyst was changed to 5 wt% of SGO loading, which is attributed to the increase in the reactive site and sorption capacity of SGO [30]. However, the furfural yield was observed to significantly decline to 16.0 % with the increases in the catalyst loading in the reaction system. This could be explained that the formation of the by-product was unavoidable if the excessive solid acid SGO was used. Particularly, humin, one kind of low-value solid compound with a complex structure, was stated too strongly diminishes the yield of valuable platform chemicals from the hydrolysis of biomass [31]. Under the suitable condition, those compounds were possibly formed by the resinification, polycondensation, and cyclization that occurred among the resultant furfural themselves or between furfural and xylose based on the aldol condensation [32]. Therefore, in this work, the amount of hemicellulose was utilized with 5 wt% SGO to maximize the sufficient acidic site for hydrolysis reaction and restrict the acidic-favored formation of any unwanted products. The highest furfural efficiency due to the use of 5 % SGO could confirm the impressive catalytic capacity of SGO. For comparison with liquid mineral acid under the same condition, the large amount of those catalysts were used due to the high concentration of protons in aqueous media that have consequently come up against various difficulties in residue neutralization and treatment for recovery and disposal after the reaction. The requirement of a minimal amount of catalyst not only guarantees a high reaction efficiency but also effectively simplifies the reaction and operating process [30].

Toward the thermochemical liquefaction, the temperature was deemed as a vital parameter that affects the production of furfural. According to Figure 8b, the yield was obtained 4.4 and 10.2 % at 150 and 170 °C, respectively, and once running temperature from 180 to 200 °C, the yield increased sharply. This is due to the higher temperature that can accelerate the dehydration processes of the hemicellulose to xylose and from xylose to furfural [33]. Besides, according to the research of Weingarten et al (2010), the dehydration of xylose requires the highest activation energy, so temperature plays a vital role in the improvement of the yield [34]. The hydrolysis reaction as a dominant process held up a maximum furfural yield at 190 °C (20.6 %), but the considerable decline to 12.1 % expressed in the temperature range 200–230 °C. The yield loss was strongly believed to be caused by the conversion of the desired product to other furan derivatives under the acidic medium at high temperatures [35]. Besides, the reduction of the various functionalized group such as –OH, –COOH, or –$PhSO_3H$ in SGO during the hydrolysis process could decline its catalytically

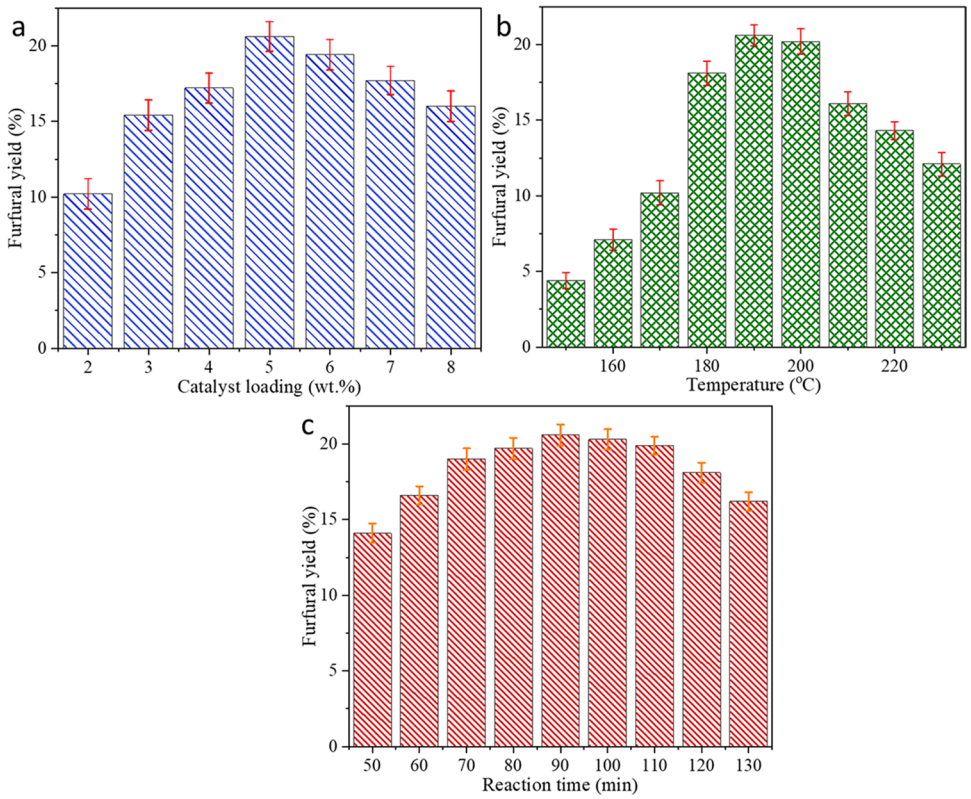

Fig. 8 Effect of **a** catalyst loading, **b** temperature, and **c** reaction time on the furfural yield

acidic sites via the catalytic capacity corresponding to the major loss in furfural yield [36, 37]. Therefore, it is worth noting that the yield of 20.6% was appropriately optimized at 190 °C to obtain the desired product. Compared to other research toward the energy-consuming duty, these results were noticed as impressive as the reaction with high furfural yield was only operated at the low temperature using the environmentally friendly catalyst.

The impact of reaction time on furfural yield was studied in the range of 50–130 min, as shown in Figure 8c. The furfural yield is observed to increase to 19.0 % when the reaction was occupied to 70 min and reach the peak (20.6 %) after the 90-min process. However, the result subsequently attested a drop to 16.2 % after 130 min. This could be explained as the occurrence of competitive side reactions, especially the formation of humin as mentioned above [38, 39]. The extended retention times in the reactor along with high temperature (190 °C) can lead to undesired decomposition, condensation, and/or repolymerization among the furfural molecules and their unwanted derivatives, which aid in the decrease in yield [31]. According to Mohamad et al (2017), the dehydration of xylose to furfural was claimed to achieve a lower reaction time than that of the unfavorable reaction, i.e., the condensation and repolymerization. Therefore, a longer reaction time resulted in the vast occurrence of by-products that affect the furfural yield.

From the empirical investigation, the optimal reaction condition for synthesis furfural from biomass using SGO as an active acid catalyst was indicated as 5 wt% catalyst loading as compared with the hemicellulose dose, the temperature of 190 °C, and reaction time of 90 min.

According to Table 4, the SGO expressed a synergetic catalytic property in comparison with other mineral acids at the same condition. Besides, the extreme temperature with an extended reaction can lead to a diminish in yield due to the side reaction. It was recorded that furfural chemically contains three unsaturated bonds with highly reactive characteristics; hence, it is vital to control the furfural recovery immediately after reaction by steam distillation to avoid its interaction with other aldehydes and other aromatic compounds [41]. Furthermore, a higher concentration of proton H^+ enriched by the acidic catalyst was proved to enhance the efficiency of the hydrolysis of hemicellulose to furfural. From the table, it is concluded that the use of SGO as a catalyst is a highly promising pathway for furfural production from biomass.

The conversion from hemicellulose to furfural undergoes 2 steps: hydrolysis of hemicellulose to xylose (Figure 9) and dehydration of xylose to furfural under acidic medium (Figure 10). For the hydrolysis of hemicellulose to xylose, the oxygen-containing groups (–COOH, –OH) and $–SO_3H$ in SGO produce proton H^+, which directly attacks the C–O–C bonding to form trivalent oxygen bonding (a). This bond then is separated into 2 groups (b): one containing

Table 4 The comparison of furfural yield

Catalysts	Conditions	Yield (%)	References
SGO-5	5 wt% catalyst, 190 °C, 90 min	20.6	This research
H_2SO_4	170 °C, 0.5 wt% H_2SO_4	11.44	[2]
SGO	2 wt% catalyst, 200 °C, 35 min	62*	[30]
H_2SO_4	5 wt% catalyst, 190 °C, 90 min	59**	[21]
GO-SO_3H	5 wt% catalyst, 190 °C, 90 min	86**	[21]
H_2SO_4	2 wt% catalyst, 110 °C, 90 min	16.35	[40]

*Yield based on the xylose used

**Yield based on the xylan used

carbocation, which later reacts with a water molecule to yield –C–O^+H_2, and one containing hydroxyl –OH group (c). The –C–O^+H_2 is deprotonated to form –C–OH bonding (d). Following the dehydration process of xylose, the H^+ from SGO will react with the 4th OH group of xyloses forming a trivalent oxygen bonding –C–O^+H_2. Due to the lower electronegativity, the charge was transferred to the nearby carbon to form a –C^+H cation and release one water molecule (a). Next, the 4th and 5th carbon will create C=C bonding, which leads to the ring opening and the formation of C=O at 1st carbon (b). Likewise, the H^+ continues

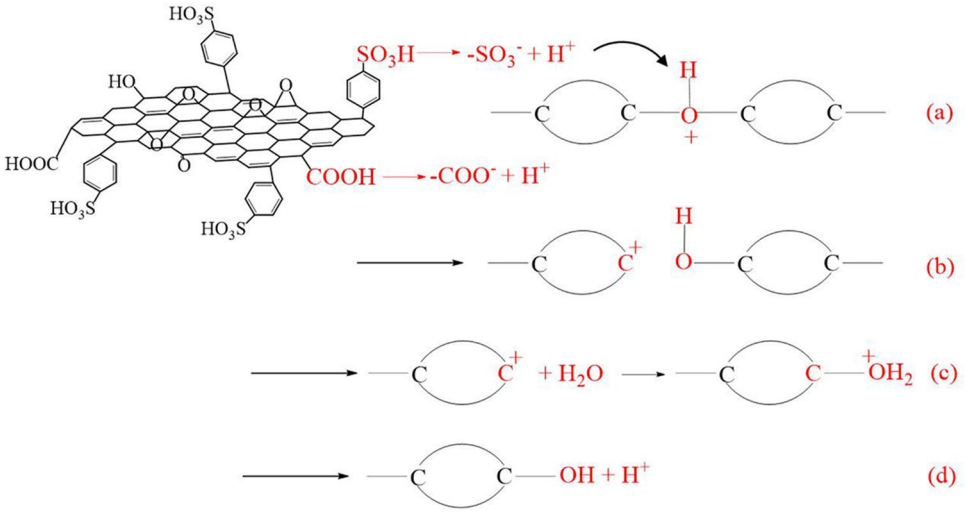

Fig. 9 The hydrolysis mechanism of SGO

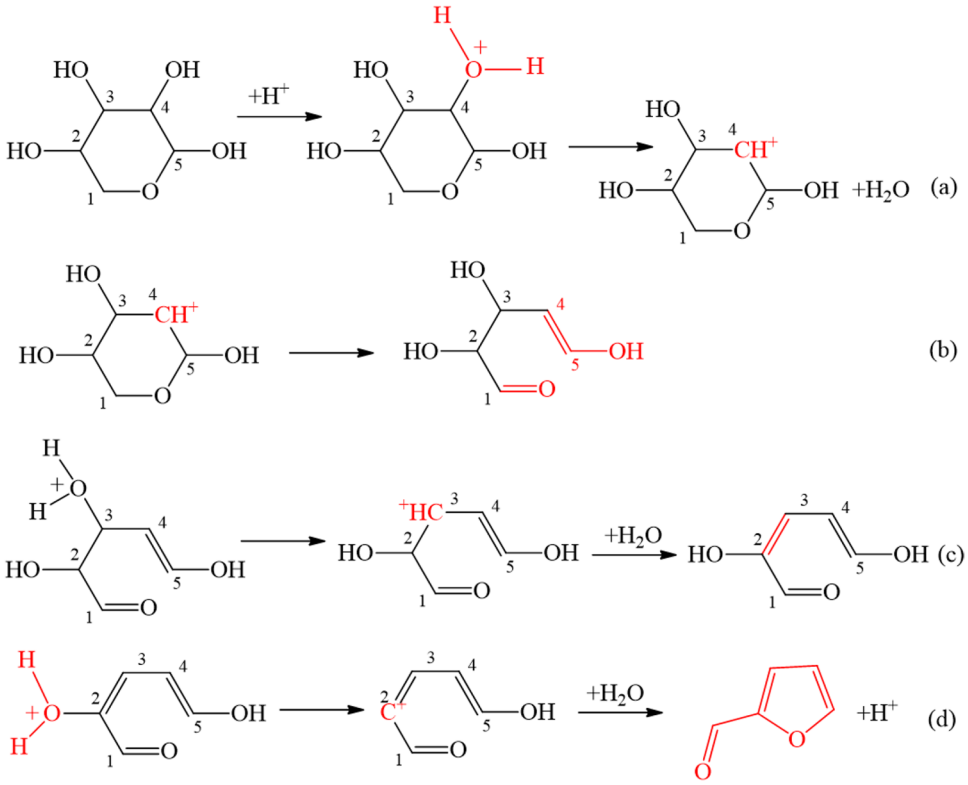

Fig. 10 The dehydration mechanism of furfural

to attack with the OH group at 3rd carbon to yield another double bond and release water (c). Eventually, the proton will react with the OH group at 2nd carbon, attributing to deprotonation to close the ring of furfural (d).

4 Conclusions

In this study, furfural was synthesized from sugarcane bagasse, a common by-product in agriculture, as a raw material to solve the problem of handling biomass as well as maintaining the sustainable furfural supply for industries. Besides, sulfonated graphene oxide (SGO) catalyst with GO:SA precursor ratio of 1:3.5, corresponding to SGO-5 sample, shows the highest catalytic performance. SGO-5 is a rapid and efficient catalyst with a low catalyst loading (5 wt% as compared with the hemicellulose used) for 90 min at 190 °C highest conversion of furfural from this biomass resources. Based on the characterization of SGO-5 also has $–PhSO_3H$ groups substitution, which is a major factor in the acidity of the material and ensures good exfoliation of GO layers of the material as well as participates in the hydrolysis of hemicellulose and dehydrates xylose to form furfural. Furthermore, the sulfonation of GO makes the catalyst more reactive in the aqueous phase and also stabilizes other acidic functional groups such as –COOH and –C–OH of GO, which increases the catalytic efficiency at the right conditions.

Acknowledgements We acknowledge the support of time and facilities from Ho Chi Minh City University of Technology (HCMUT), VNU-HCM for this study.

Author contribution Le Minh Huong, Ninh Thi Tinh, Tran Quoc Trung, Nguyen Quoc Viet, and Nguyen Minh Dat: Experimental, Data curation and Formal analysis; Nguyen Thi Phuong and Tran Thanh Tuan: Writing-Original draft and Editing; Do Gia Nghiem, Doan Ba Thinh, and Doan Thi Yen Oanh: Writing-Review and Editing; Hoang Minh Nam, Mai Thanh Phong, and Nguyen Huu Hieu: Conceptualization and Methodology, Supervision.

Data availability Not applicable.

Declarations

Conflict of interest The authors declare no competing interests.

References

1. Santos C, Bueno D, Sant'Anna C, Brienzo M (2020) High xylose yield from stem and external fraction of sugarcane biomass by diluted acid pretreatment. Biomass Convers Biorefinery:1–9. https://doi.org/10.1007/s13399-020-01088-z
2. Ntimbani RN, Farzad S, Görgens JF (2021) Furfural production from sugarcane bagasse along with co-production of ethanol from furfural residues. Biomass Convers Biorefinery:1–11. https://doi.org/10.1007/s13399-021-01313-3
3. Wang J, Wang J, Yu Y (2021) Effective and safer catalyst KHSO4 for producing furfural: a platform compound. Biomass Convers Biorefinery 11:1293–1300
4. Oefner PJ, Lanziner AH, Bonn G, Bobleter O (1992) Quantitative studies on furfural and organic acid formation during hydrothermal, acidic and alkaline degradation of D-xylose. Monatshefte Für Chemie Chem Mon 123:547–556. https://doi.org/10.1007/BF00816848
5. Danon B, Hongsiri W, van der Aa L, de Jong W (2014) Kinetic study on homogeneously catalyzed xylose dehydration to furfural in the presence of arabinose and glucose. Biomass Bioenergy 66:364–370. https://doi.org/10.1016/j.biombioe.2014.04.007
6. Delbecq F, Wang Y, Muralidhara A, El Ouardi KE, Marlair G, Len C (2018) Hydrolysis of hemicellulose and derivatives-a review of recent advances in the production of furfural. Front Chem 6. https://doi.org/10.3389/fchem.2018.00146
7. Agirrezabal-Telleria I, Gandarias I, Arias PL (2014) Heterogeneous acid-catalysts for the production of furan-derived compounds (furfural and hydroxymethylfurfural) from renewable carbohydrates: a review. Catal Today 234:42–58. https://doi.org/10.1016/j.cattod.2013.11.027
8. Ma J, Li W, Guan S, Liu Q, Li Q, Zhu C, Yang T, Ogunbiyi AT, Ma L (2019) Efficient catalytic conversion of corn stalk and xylose into furfural over sulfonated graphene in γ-valerolactone. RSC Adv 9:10569–10577. https://doi.org/10.1039/c9ra01411j
9. Van Bao H, Dat NM, Giang NTH, Thinh DB, Trinh DN, Hai ND, Khoa NAD, Nam HM, Phong MT, Hieu NH (2021) Behavior of ZnO-doped TiO2/rGO nanocomposite for water treatment enhancement. Surf Interfaces 23:100950
10. Diep TC, Dat NM, Tai LT, Phuc NHT, An NTT, Huong LTT, Hung NG, Hy LD, Oanh DTY, Nam HM (2020) Synthesis of graphene oxide-based silver cotton fabric application for antibacterial activity. Vietnam J Chem 58:844–850
11. Dat NM, Quan TH, Anh TNM, Thinh DB, Diep TC, Hai ND, Khang PT, Nam HM, Phong MT, Hieu NH (2021) Hybrid graphene oxide-immobilized silver nanocomposite with optimal fabrication route and multifunctional application. Appl Surf Sci 551:149434
12. Trung T, Thinh D et al (2020) Synthesis of furfural from sugarcane bagasse by hydrolysis method using magnetic sulfonated graphene oxide catalyst. Wiley Online Libr 2020:245–250. https://doi.org/10.1002/vjch.201900180
13. Wang C, Zhang L, Zhou T, Chen J, Xu F (2017) Synergy of Lewis and Brønsted acids on catalytic hydrothermal decomposition of carbohydrates and corncob acid hydrolysis residues to 5-hydroxymethylfurfural. Sci Rep 7:1–9. https://doi.org/10.1038/srep40908
14. Si Y, Samulski ET (2008) Synthesis of water soluble graphene. Nano Lett 8:1679–1682. https://doi.org/10.1021/NL080604H
15. Bao HV, Dat NM, Giang NTH, Thinh DB, Tai LT, Trinh DN, Hai ND, Khoa NAD, Huong LM, Nam HM, Phong MT, Hieu NH (2021) Behavior of ZnO-doped TiO2/rGO nanocomposite for water treatment enhancement. Surf Interfaces 23:100950. https://doi.org/10.1016/j.surfin.2021.100950
16. Li X, Shu R, Wu Y, Zhang J, Wan Z (2021) Fabrication of nitrogen-doped reduced graphene oxide/cobalt ferrite hybrid nanocomposites as broadband electromagnetic wave absorbers in both X and Ku bands. Synth Met 271:116621. https://doi.org/10.1016/j.synthmet.2020.116621
17. Gong Y, Li D, Fu Q, Pan C (2015) Influence of graphene microstructures on electrochemical performance for supercapacitors. Prog Nat Sci Mater Int 25:379–385. https://doi.org/10.1016/j.pnsc.2015.10.004
18. Thinh DB, Tu TH, Dat NM, Hong TT, Cam PTN, Trinh DN, Nam HM, Phong MT, Hieu NH (2021) Ice segregation induced self-assembly of graphene oxide into graphene-based aerogel for

enhanced adsorption of heavy metal ions and phenolic compounds in aqueous media. Surf Interfaces 26:101309
19. Dang NH, Tu TH, Linh VNP, Thy LTM, Nam HM, Phong MT, Hieu NH (2019) Preparation of magnetic iron oxide/graphene aerogel nanocomposites for removal of bisphenol A from water. Synth Met 255:116106
20. Ayyaru S, Ahn YH (2017) Application of sulfonic acid group functionalized graphene oxide to improve hydrophilicity, permeability, and antifouling of PVDF nanocomposite ultrafiltration membranes. J Membr Sci 525:210–219. https://doi.org/10.1016/j.memsci.2016.10.048
21. Upare PP, Hong DY, Kwak J, Lee M, Chitale SK, Chang JS, Hwang DW, Hwang YK (2019) Direct chemical conversion of xylan into furfural over sulfonated graphene oxide. Catal Today 324:66–72. https://doi.org/10.1016/j.cattod.2018.07.002
22. Duong NT, An TB, Thao PT, Oanh VK, Truc TA, Vu PG, Hang TTX (2020) Corrosion protection of carbon steel by polyurethane coatings containing graphene oxide. Vietnam J Chem 58:108–112
23. Naeim-Fallahiyeh S, Rostami E, Golchaman H, Kaman-Torki S (2020) Graphene oxide anchored with sulfonic acid-functionalized glycerin: production, characterization and catalytic performance for the synthesis of N,N′-alkylidene bisamides. Res Chem Intermed 46:4141–4153. https://doi.org/10.1007/s11164-020-04197-6
24. Ng SW, Noor N, Zheng Z (2018) Graphene-based two-dimensional Janus materials. NPG Asia Mater 10:217–237. https://doi.org/10.1038/s41427-018-0023-8
25. Eigler S, Dotzer C, Hof F, Bauer W, Hirsch A (2013) Sulfur species in graphene oxide. Chemistry. 19:9490–9496. https://doi.org/10.1002/chem.201300387
26. Huong NT, Dat NM, Thinh DB, Minh Anh TN, Nguyet DM, Quan TH, Bao Long PN, Nam HM, Phong MT, Hieu NH (2020) Optimization of the antibacterial activity of silver nanoparticles-decorated graphene oxide nanocomposites. Synth Met 268:116492. https://doi.org/10.1016/j.synthmet.2020.116492
27. Swami M, Mathpati S, Ghuge H, Patil S (2017) Eco-friendly highly efficient solvent free synthesis of benzimidazole derivatives over sulfonic acid functionalized graphene oxide in ambient condition. Res Chem Intermed 43:2033–2053. https://doi.org/10.1007/s11164-016-2745-y
28. Ossonon BD, Bélanger D (2017) Synthesis and characterization of sulfophenyl-functionalized reduced graphene oxide sheets. RSC Adv 7:27224–27234. https://doi.org/10.1039/C6RA28311J
29. Upare PP, Yoon J-W, Kim MY, Kang H-Y, Hwang DW, Hwang YK, Kung HH, Chang J-S (2013) Chemical conversion of biomass-derived hexose sugars to levulinic acid over sulfonic acid-functionalized graphene oxide catalysts. Green Chem 15:2935–2943
30. Lam E, Chong JH, Majid E, Liu Y, Hrapovic S, Leung ACW, Luong JHT (2012) Carbocatalytic dehydration of xylose to furfural in water. Carbon N Y 50:1033–1043. https://doi.org/10.1016/j.carbon.2011.10.007
31. Köchermann J, Schreiber J, Klemm M (2019) Conversion of d-xylose and hemicellulose in water/ethanol mixtures. ACS Sustain Chem Eng 7:12323–12330. https://doi.org/10.1021/acssuschemeng.9b01697
32. Shi N, Liu Q, Cen H, Ju R, He X, Ma L (2020) Formation of humins during degradation of carbohydrates and furfural derivatives in various solvents. Biomass Convers Biorefinery 10:277–287. https://doi.org/10.1007/s13399-019-00414-4
33. Möller M, Schröder U (2013) Hydrothermal production of furfural from xylose and xylan as model compounds for hemicelluloses. RSC Adv 3:22253–22260. https://doi.org/10.1039/c3ra43108h
34. Weingarten R, Cho J, Conner Wm J, Curtis GWH (2010) Kinetics of furfural production by dehydration of xylose in a biphasic reactor with microwave heating. Green Chem 12:1423–1429. https://doi.org/10.1039/C003459B
35. Kim ES, Liu S, Abu-omar MM, Mosier NS (2012) Selective conversion of biomass hemicellulose to furfural using maleic acid with microwave heating. Energy Fuels 26:1298–1304. https://doi.org/10.1021/ef2014106
36. Hayes W, Joseph P et al (n.d.) Production of reduced graphene oxide via hydrothermal reduction in an aqueous sulphuric acid suspension and its electrochemical behaviour, Springer. https://doi.org/10.1007/s10008-014-2560-6
37. Zhou Y, Bao Q, Tang L et al (2009) Hydrothermal dehydration for the "green" reduction of exfoliated graphene oxide to graphene and demonstration of tunable optical limiting properties. ACS Publ 21:2950–2956. https://doi.org/10.1021/cm9006603
38. Mamman AS, Lee JM, Kim YC, Hwang IT, Park NJ, Hwang YK, Chang JS, Hwang JS (2008) Furfural: Hemicellulose/xylose-derived biochemical, Biofuels. Bioprod Bioref 2:438–454. https://doi.org/10.1002/BBB.95
39. Pholjaroen B, Li N, Wang Z, Wang A, Zhang T (2013) Dehydration of xylose to furfural over niobium phosphate catalyst in biphasic solvent system. J Energy Chem 22:826–832. https://doi.org/10.1016/S2095-4956(14)60260-6
40. Uppal SK, Gupta R, Dhillon RS, Bhatia S (2008) Potential of sugarcane bagasse for production of furfural and its derivatives. Sugar Tech 10:298–301
41. Mao L, Zhang L, Gao N, Li A (2012) FeCl 3 and acetic acid co-catalyzed hydrolysis of corncob for improving furfural production and lignin removal from residue. Bioresour Technol 123:324–331. https://doi.org/10.1016/j.biortech.2012.07.058